

# Investigation of the Machining Parameters and the Environment of Polyamide 6 on Surface Roughness Using Experimental and Statistical Methods

**Wael H. A. Shaheen**

Department of Automated Manufacturing Engineering, Al-Khwarizmi College of Engineering, University of Baghdad, Baghdad, Iraq  
waelshaheen@kecbu.uobaghdad.edu.iq

**Marwan Salman**

Department of Automated Manufacturing Engineering, Al-Khwarizmi College of Engineering, University of Baghdad, Baghdad, Iraq  
marwan@kecbu.uobaghdad.edu.iq

**Moneer H. Tolephih**

Al-Naji University, Baghdad, Iraq  
monerht@alNaji-uni.edu.iq (corresponding author)

**Thamir Alsharifi**

Department of Automated Manufacturing Engineering, Al-Khwarizmi College of Engineering, University of Baghdad, Baghdad, Iraq  
thamirha@kecbu.uobaghdad.edu.iq

**Wassan S. Abd Al-Sahb**

Department of Mechanical Engineering, College of Engineering, University of Baghdad, Baghdad, Iraq  
wassan.safaa@coeng.uobaghdad.edu.iq

**Oday I. Abdullah**

Department of Energy Engineering, College of Engineering, University of Baghdad, Baghdad, Iraq | College of Engineering, Al-Naji University, Baghdad, Iraq | Department of Mechanics, Al-Farabi Kazakh National University, Almaty, Kazakhstan  
oday.abdullah@tuhh.de

Received: 6 July 2025 | Revised: 1 August 2025 and 25 August 2025 | Accepted: 30 August 2025

Licensed under a CC-BY 4.0 license | Copyright (c) by the authors | DOI: <https://doi.org/10.48084/etasr.13208>

## ABSTRACT

This study investigates experimentally and statistically the influences of the Machining Parameters (MPs) and environments on the surface roughness ( $R_a$ ) of Polyamide 6 (PA6) during the turning operation. The experiments were conducted using a lathe machine, carbide cutting tool, and roughness tester. The statistical approach was implemented using Taguchi Experiment Design (TED) and Analysis of Variance (ANOVA). The parameters and their values were: cutting velocity ( $V_c$ ) of 125, 200, and 250 m/min; feed rate ( $F_R$ ) of 0.05, 0.1, and 0.15 mm/rev; and cutting depth ( $D_C$ ) of 2, 4, and 6 mm. The environments used were: dry (D), compressed air (A), and air-water mixture (A+W). The research aimed to improve the cutting surface quality of PA6 based on the  $R$  criterion. The results revealed that the  $F_R$  is the most influential factor on  $R$  compared to other factors. The effect percentages on  $R$  were 61%, 15%, 13%, and 11% for  $F_R$ , Machining Environments (MEs),  $D_C$ , and  $V_C$ , respectively. The optimum combination has been

achieved based on an  $F_R$  of 0.05 mm/rev, air with water, a  $D_C$  of 2 mm, and a  $V_C$  of 125 m/min, providing a minimum total average surface roughness ( $R_a$ ) of 1.2  $\mu\text{m}$  for PA6. The study demonstrates that an optimum combination can enhance the cutting surface quality, reduce the machining costs, and provide a pathway for producing high-performance PA6 components.

**Keywords**-Polyamide 6; cutting velocity; feed rate; cutting depth; machining environment; surface roughness; Taguchi design; ANOVA

## I. INTRODUCTION

Plastic is a vital component of daily life, with plastic products ranging from high-technology items, like prosthetic hip and knee joints, to throw-away food containers [1]. One of the factors contributing to the widespread use of plastic in a variety of industrial applications is its wide range of properties and ease of processing [2]. Most plastic products in the market are manufactured using the molding process, but there is often a need for plastic parts with specific shapes and in small quantities, especially in the engineering field [3]. The molding process is not economically feasible due to the high costs of mold manufacturing; therefore, various operating processes, such as turning and milling, are employed to produce these parts [4]. PA6 is a thermoplastic material of the nylon polymer family known for its excellent mechanical and thermal properties [5]. It is a semi-crystalline polymer, meaning that under appropriate cooling conditions its molecules can arrange into ordered crystalline regions embedded within an amorphous matrix [6]. This structure contributes to its unique combination of strength, toughness, and thermal stability [7]. The semi-crystalline structure and low thermal conductivity of PA6 pose challenges during machining, particularly in achieving an optimal surface finish and minimizing the tool wear [8]. Research has employed different plastic materials and has relied on the surface roughness ( $R_a$ ) to evaluate their results, due to the importance of this variable in expressing the quality of the processed surfaces. Authors in [9] studied the effect of optimal variables, including spindle speed, feed rate ( $F_R$ ), and cutting depth ( $D_C$ ) on the Tool Life (TL), surface roughness ( $R_a$ ), and Material Removal Rate (MRR) of Polyoxymethylene (POM) in the TP using Taguchi Experiment Design (TED) and Analysis of Variance (ANOVA). Authors in [10] investigated the influence of the cutting tool metal type on  $R_a$  and cutting force ( $F_C$ ) for polytetrafluoroethylene using TED. Authors in [11] deployed the Response Surface Methodology (RSM) to optimize the cutting velocity ( $V_C$ ),  $F_R$ , and  $D_C$  for decreasing the  $R_a$  and increasing the MRR when machining POM. Authors in [12] experimentally found that the  $D_C$  is the most influential parameter on the  $R_a$  of high-density polyethylene, and  $V_C$  is the most effective variable on the  $R_a$  of PA6. Authors in [13] studied the prediction methodology of  $R_a$  for PA utilizing an artificial neural network in the milling operation, taking the Machining Parameters (MPs) and humidity conditions into consideration. Authors in [14] used TED and ANOVA to study and optimize the  $V_C$ ,  $F_R$ ,  $D_C$ , and cutting tool rake angle for reducing the cutting forces and geometry deformation of aluminum products. Authors in [15] studied the effect of pointed, relief, lead, and edge radius angles of cutting tools on the  $R_a$  of PA6 in the TP, utilizing high-speed steel cutting tool, TED, and ANOVA. The optimization and the effect of the edge radius angle and nose radius of the cutting tool on the  $F_C$  of cast nylon 6 have been investigated in [16] using TED and

ANOVA. Authors in [17] studied the influence of the nozzle diameter and raster angle on the mechanical properties of 3D printed nylon-carbon fibers using fused deposition modeling. Authors in [18] studied the effect of  $V_C$ , sheet metal temperature, and punch edge radius on the copper product deformation using the numerical approach.

The impact of different parameters on selected materials has been investigated using various techniques, including statistical, numerical, and artificial intelligence. However, shortcomings were found in previous research, regarding the minimization of the  $R_a$  of PA6 under high cutting quality, the limited improvement percentages in PA6 quality, and the analysis of the effect percentages of MPs and MEs on PA6. Therefore, the current study addresses this research gap by investigating the influence of selected MPs and MEs on the  $R_a$  of PA6 in the TP. This research focuses on reducing the  $R_a$  of PA6 by managing MPs, including  $F_R$ ,  $D_C$ ,  $V_C$ , and MEs, such as dry (D), compressed air (A), and air-water mixture (A+W). The Design of Experiments (DOE), TED, and ANOVA were applied to achieve the research objectives. The aim of the present study is to determine the most influential parameter and environment on the  $R_a$  of PA6.

## II. RESEARCH METHODOLOGY

### A. Materials and Experimental Design

The PA6 was chosen as a material for this study, with its physical properties being summarized in Table I [19]. A PA6 rod with a diameter of 40 mm and a length of 500 mm was used in experiments. Samples of 30 mm length were prepared for the testing. The experiments were designed using the Taguchi L9 orthogonal array, which entails four parameters, including  $V_C$ ,  $F_R$ ,  $D_C$ , and MEs (D, A, and A+W), as shown in Table II. The Taguchi L9 orthogonal array was chosen because it enables the efficient optimization of multiple parameters (factors) with fewer experiments while maintaining the statistical reliability. Specifically, this study used four factors with three levels each, and the L9 array was a well-established design for such situations, balancing experimental effort and robustness.

TABLE I. PHYSICAL PROPERTIES OF PA6

Property	Value	Unit
Density	1.14	$\text{g/cm}^3$
Water absorption at balance	2.6	%
Melting point	223	$^\circ\text{C}$
Thermal conductivity	0.24	$\text{W/m.K}$
Tensile strength	45-85	MPa
Heat deflection temperature at 0.46 MPa load	170-180	$^\circ\text{C}$
Heat deflection temperature at 1.8 MPa	55-65	$^\circ\text{C}$
Glass transition temperature	60	$^\circ\text{C}$

The MP and ME values were chosen based on previous literature and experimental tests to obtain better results in terms of lower  $R_a$  of PA6.

TABLE II. MPs OF USED SAMPLES

MPs (unit)	Level 1	Level 2	Level 3
$D_C$ (mm)	2	4	6
$F_R$ (mm/rev)	0.05	0.1	0.15
$V_C$ (m/min)	125	200	250
MEs	A	A+W	D

### B. Experimental Setup

The experiments were conducted deploying a CU-500 lathe, with its specifications being listed in Table III. A carbide cutting tool, Mitsubishi CNMG 120408 UE6020, and a PCLNR 2525 M12 tool holder were used for machining. A custom-designed cooling system was employed to create different MEs, including D, A, and A+W. The SRT5000 roughness tester was used to measure  $R_a$ .

TABLE III. SPECIFICATIONS OF THE LATHE MACHINE

Specifications	Values
Number of velocities of the rotating head	21
Rotary head velocity range	20-2000 rpm
Engine power	7.5 KW
Longitudinal feeding field	0.04-12 mm/rev
Occasional feeding field	0.02-6 mm/rev

### C. Statistical Methods

The flowchart for the research methodology is presented in Figure 1. TED is a robust statistical approach for designing experiments that evaluate the impact of multiple factors simultaneously. This method is particularly useful for optimizing processes and products to be insensitive to uncontrollable factors while maintaining the cost-effectiveness [20]. DOE is a systematic method employed to determine the most effective set of experiments for studying complex processes. By conducting experiments at different levels of these factors, TED minimizes the number of trials while maximizing the predictive knowledge of the process [21]. The Signal-to-Noise Ratio (SNR) is a key metric in the TED analysis, calculated to assess the influence of MPs on  $R_a$ . For  $R_a$ , the "smaller is better" criterion is applied, as lower roughness values indicate better surface quality. The SNR and average  $R_a$  can be calculated using (1) and (2) [22]. The latter can be applied to determine the optimum combination of MPs that yield the closest to ideal  $R_a$  values [11]. The delta value is calculated as the difference between the largest and smallest average values of SNR for each factor. The factors are then ranked based on their delta values, with the highest delta indicating the most significant influence on  $R_a$  [23]. The ANOVA is used to quantify the percentage of contribution of each MP to  $R_a$ . The ANOVA equations are [16-18]:

$$SNR = -10 \log_{10} \left( \frac{1}{n} \sum_{i=1}^n y_i^2 \right) \quad (1)$$

$$R_a = \frac{1}{n} \sum_{i=1}^n |y_i| = \frac{1}{n} \sum (y_1^2 + y_2^2 + y_3^2) \quad (2)$$

$$m = \frac{1}{n} \sum_{i=1}^n n_i \bar{x}_i \quad (3)$$

$$TSS = \sum \bar{x}_i^2 \quad (4)$$

$$SSM = n \times m^2 \quad (5)$$

$$NOS = TSS - SSM \quad (6)$$

$$DOF = NOS - 1 \quad (7)$$

$$SSF = n[(A_1 - m)^2 + (A_2 - m)^2 + (A_3 - m)^2] \quad (8)$$

$$MS = \frac{SSF}{DOFF} \quad (9)$$

$$POC = \frac{100 \times SSF}{TSS} \quad (10)$$

where  $y_i$  is the surface roughness value at the  $i^{th}$  test,  $m$  is the overall mean of samples,  $n$  is the number of samples or experiments, and  $n_i$  is the sample size.  $\bar{x}_i$  is  $i^{th}$  sample mean,  $TSS$  is the total sum of squares,  $SSM$  is the sum of squares due to mean,  $NOS$  is the number of stages of a variable  $i$ ,  $DOF$  is the degree of freedom,  $SSF$  is the sum of squares for factor,  $A_1$ ,  $A_2$ , and  $A_3$  are arithmetic mean of  $SN$  for a variable  $i$  at level 1, 2, and 3, respectively,  $MS$  is the mean of squares,  $DOFF$  is the degree of freedom for factor  $A_1$ ,  $A_2$ , and  $A_3$ , and  $POC$  is the percentage of contribution.

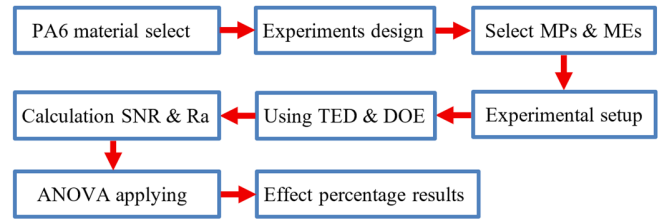


Fig. 1. Flowchart of the research methodology.

## III. RESULTS AND DISCUSSION

### A. Results

The SNR was calculated using the smaller-is-better criteria. For each MP, the SNR values at the three test levels were computed using (1), and the results are displayed in Table IV. Equation (2) was utilized to obtain the three levels of  $R_a$ , including  $R_{a1}$ ,  $R_{a2}$ , and  $R_{a3}$  of PA6, and the outcomes are presented in Table IV. The data in Table IV can be shown by different figures, where each point on the chart represents one stage of the studied parameter. This means that each point practically represents 3 samples or experiments. The  $R_{a1}$ ,  $R_{a2}$ , and  $R_{a3}$  of each sample are summed and then divided by three to obtain the total  $R_a$  for each sample.

### B. Discussion

Figures 2(a) and 2(b) illustrate the relationships between the  $V_C$  and total  $R_a$  at  $D_C$  values of 2, 4, and 6 mm and at  $F_R$  values of 0.05, 0.1, and 0.15 mm/rev. It is indicated that the low  $V_C$  values of 125 and 200 m/min result in minimum total  $R_a$  values of 1.2  $\mu\text{m}$  at  $D_C$  of 2 mm and  $F_R$  values of 0.05 and 0.1 mm/rev. In contrast, the high  $V_C$  value of 250 m/min results in a maximum total  $R_a$  of 2.5  $\mu\text{m}$  at  $D_C$  of 2 mm and  $F_R$  of 0.15 mm/rev. When using low  $V_C$ , the turning tool requires a long time to contact and cut the PA6, which leads to a minimal burr formation on the finished product and results in better surface quality with the lowest  $R_a$ .

TABLE IV.  $R_a$  AND SNR USING TED METHOD

Sample no.	MP				Test results			Total	SNR
	$V_C$ (m/min)	$F_R$ (mm/rev)	$D_c$ (mm)	MEs	$R_{a1}$ ( $\mu\text{m}$ )	$R_{a2}$ ( $\mu\text{m}$ )	$R_{a3}$ ( $\mu\text{m}$ )	$R_a$ ( $\mu\text{m}$ )	
1	125	0.05	2	A	1.30	1.10	1.18	1.2	-1.556
2	200	0.10	2	A+W	1.05	1.23	1.20	1.2	-1.309
3	250	0.15	2	D	2.60	2.32	2.45	2.5	-7.816
4	200	0.05	4	D	1.59	1.46	1.76	1.6	-4.126
5	250	0.10	4	A	2.00	2.40	2.07	2.2	-6.704
6	125	0.15	4	A+W	1.92	1.94	2.08	2.0	-5.939
7	250	0.05	6	A+W	1.22	1.12	1.31	1.2	-1.721
8	125	0.10	6	D	1.39	1.43	1.24	1.4	-2.644
9	200	0.15	6	A	2.40	2.27	2.34	2.3	-7.374

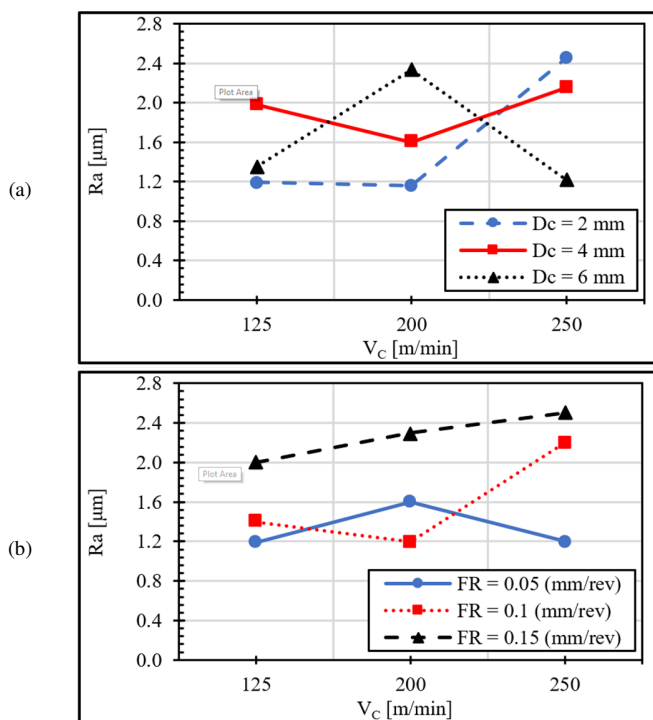


Fig. 2. Relationship between  $V_C$  and total  $R_a$  at various: (a)  $D_c$ , (b)  $F_R$ .

A high  $V_C$  increases the friction between the turning tool and product, raising the temperature, which lowers the final product quality, resulting in the highest  $R_a$ . It also increases the wear of the turning tool, leading to decreased TL. It also increases the  $F_C$  and vibration, thus reducing the surface finish of PA6. In contrast, a low  $V_C$  results in lower  $F_C$  and vibration, improving the surface finish of PA6. A low  $V_C$  also lowers the wear, leading to increased TL.

Figures 3(a) and 3(b) illustrate the relationships between the  $F_R$  and total  $R_a$  at  $D_c$  values of 2, 4, and 6 mm and at  $V_C$  values of 125, 200, and 250 m/min. It is observed that the low  $F_R$  values of 0.05 and 0.1 mm/rev result in the lowest total  $R_a$  value of 1.2  $\mu\text{m}$  at a  $D_c$  value of 2 mm and at  $V_C$  values of 125 and 200 m/min. The high  $F_R$  of 0.15 mm/rev leads to the highest total  $R_a$  of 2.5  $\mu\text{m}$  at  $D_c$  of 2 mm and  $V_C$  of 250 m/min.

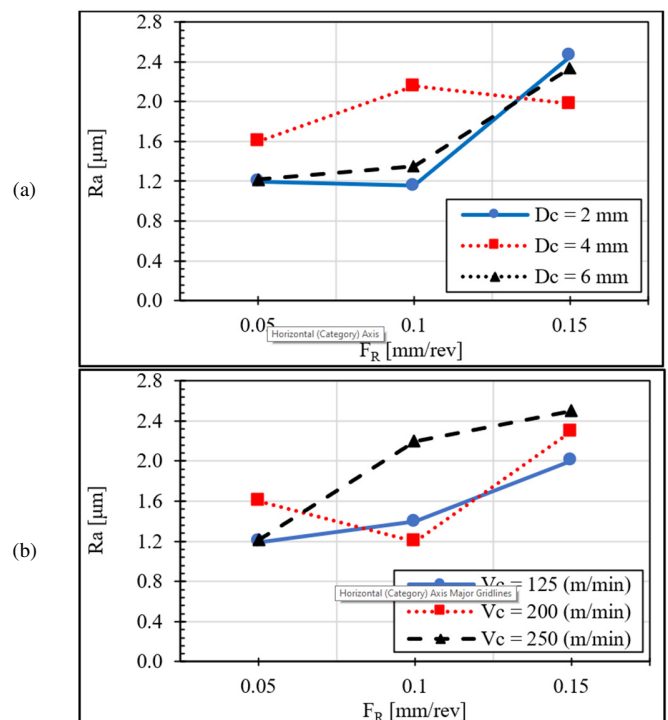


Fig. 3. Relationship between  $F_R$  and total  $R_a$  at various: (a)  $D_c$ , (b)  $V_C$ .

A low  $F_R$  leads to a higher surface quality under the lowest surface roughness of PA6. It causes the turning tool to move slowly across the PA6 workpiece during the machining process, resulting in a smooth surface finish. In contrast, a high  $F_R$  makes the tool move faster, leading to a rough surface finish. A low  $F_R$  also reduces the friction and temperature at the interface of the turning tool, resulting in smaller PA6 deformation and better surface finish. A high  $F_R$  increases the friction and temperature, leading to higher deformation and lower surface quality.

A low  $F_R$  increases the contact time on the PA6, resulting in high accuracy and improved surface finish of the material. A high  $F_R$  reduces the control over the PA6 chip formation, leading to excessive tearing of the product and resulting in low cutting quality. A low  $F_R$  decreases the vibration during the turning operation, which leads to better surface quality. In contrast, a high  $F_R$  increases the vibration, which reduces the surface quality. A low  $F_R$  offers a longer time to the control

system during the turning operation, allowing a better adjustment of the turning tool, which leads to more precision of the final PA6 surface.

The comparative analysis between Figures 3(a) and 3(b) focuses on the effect of  $F_R$  on  $R_a$  at different values of  $V_C$ , rather than  $D_C$  values. The specific emphasis is due to the highly sensitive relationship between the  $F_R$  and  $V_C$  compared with  $D_C$ . Figure 3(a) shows a different trend from Figure 3(b) in the  $R_a$  values at different  $F_R$ ,  $D_C$ , and  $V_C$ .

Figures 4(a) and 4(b) portray the relationships between the  $D_C$  and total  $R_a$  at  $V_C$  values of 125, 200, and 250 m/min and at  $F_R$  of 0.05, 0.1, and 0.15 mm/rev. It is demonstrated that the low  $D_C$  of 2 mm leads to a minimum total  $R_a$  of 1.2  $\mu\text{m}$  at  $V_C$  values of 125 and 200 m/min and at  $F_R$  values of 0.05 and 0.1 mm/rev. The high  $D_C$  of 6 mm results in a maximum total  $R_a$  of 2.5  $\mu\text{m}$  at a  $V_C$  of 250 m/min and at  $F_R$  of 0.15 mm/rev. The low  $D_C$  minimizes the MRR and deformation of PA6, reducing the required FC and resulting in a clean surface finish with the lowest roughness. The wear and vibration are also reduced, improving the stability of the turning tool, and resulting in a smoother surface finish.  $R_a$ , MMR, and  $F_C$  depend on MPs. A high MRR increases both  $R_a$  and  $F_C$ , while a low MRR results in lower  $R_a$  and  $F_C$ .

The average SNR percentages of each stage of the test for MPs and MEs are outlined in Table V, along with the delta and rank for each MP and ME, and the ANOVA results.  $F_R$  represents the most effective parameter on  $R_a$  compared with other parameters, as indicated by its first-rank position in Table V, at an effect percentage of 63%. As seen in Table V,  $V_C$ ,  $D_C$ , and MEs are considered close in influence at 11%, 13%, and 15%, respectively, while  $F_R$  has the largest influence. The experimental study in [12] suggests that the  $V_C$  is the most

effective variable on  $R_a$  for PA6. In contrast, in the current study, the  $V_C$  has the lowest influence on  $R_a$  compared to other variables. This difference is due to the use of various MEs (D, A, and A+W) and the corresponding trial values of  $V_C$ ,  $F_R$ , and  $D_C$ .

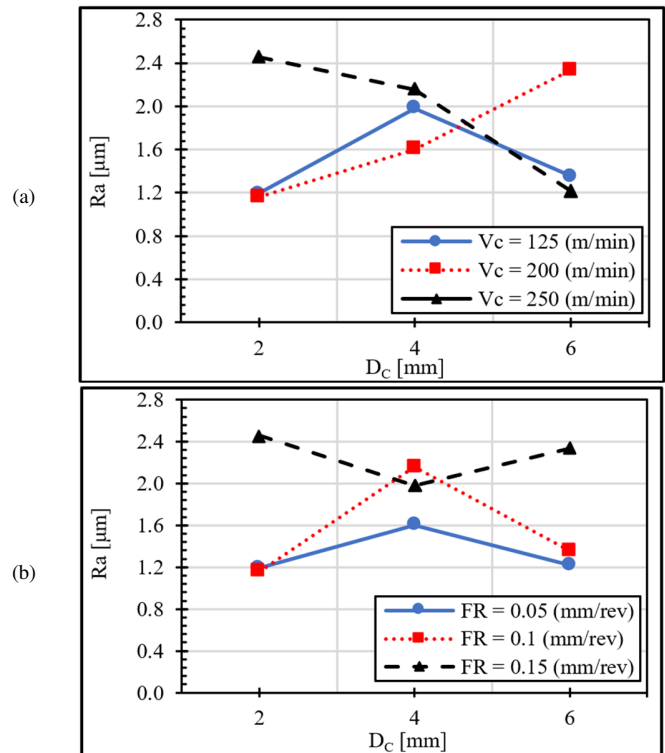


Fig. 4. Relationship between  $D_C$  and total  $R_a$  at various: (a) and  $V_C$ , (b)  $F_R$ .

TABLE V. SNR, DELTA, RANK, AND ANOVA RESULTS

MP	SNR Average percentage			Delta	Rank	ANOVA results			
	Stage 1	Stage 2	Stage 3			POC (%)	MS	TSS	DOF
$V_C$	-3.380	-4.270	-5.414	2.034	4	11	3.1200	6.2400	2
$F_R$	-2.468	-3.552	-7.043	4.576	1	61	17.147	34.293	2
$D_C$	-3.560	-5.600	-3.913	2.040	3	13	3.5280	7.0560	2
ME	-5.211	-2.990	-4.862	2.222	2	15	4.2780	8.5560	2

#### IV. CONCLUSIONS

Various studies have experimentally explored the Polyamide 6 (PA6) material without focusing on minimizing the average surface roughness ( $R_a$ ), investigating the Machining Parameters (MPs) and Machining Environments (MEs), or analyzing the impact of these factors. The present research addressed the knowledge gap of the PA6 turning process by lowering  $R_a$ , providing a comprehensive analysis of the combined effects of different MPs and MEs, and limiting the influence percentages for each parameter and all MEs using the experimental and statistical approaches. This study systematically quantified the influence of these parameters and environments to improve the quality of machined PA6 surfaces. The former successfully achieved minimum and maximum  $R_a$  values of 1.05  $\mu\text{m}$  and 2.45  $\mu\text{m}$ , respectively,

which are considered improvements over the  $R_a$  of 2.39  $\mu\text{m}$  and 11.14  $\mu\text{m}$  reported in [12].

The study highlights the critical role of MPs, including the cutting velocity ( $V_C$ ), feed rate ( $F_R$ ), cutting depth ( $D_C$ ), and MEs, such as dry (D), compressed air (A), and air-water mixture (A+W), on the  $R_a$  of PA6.  $F_R$  is indisputably the most dominant variable, contributing 61% of the overall effect. A low  $F_R$  of 0.05 mm/rev resulted in a fine finish of 1.2  $\mu\text{m}$ , while a high  $F_R$  of 0.15 mm/rev yielded a much coarser 2.5  $\mu\text{m}$  finish. The MEs were the second most dominant variable; using the A+W environment significantly improved the  $R_a$  compared with A and D. This improvement can be attributed to cooling and lubrication. The  $D_C$  and  $V_C$ , on the other hand, had much smaller effects, contributing 13% and 11%, respectively.

The current study identified the optimum parameters and environments for achieving a superior surface finish:  $V_C$  of 125 m/min,  $F_R$  of 0.05 mm/rev,  $D_C$  of 2 mm, and A+W environment. This particular combination can be utilized by manufacturers to achieve a low  $R_a$  of 1.2  $\mu\text{m}$ , which could improve the productivity and quality of the end product.

Future studies should extend this investigation to different machining operations, such as drilling, and examine its effect on the Tool Life (TL) and cutting force. Creating a predictive software simulation based on these results could also benefit the process optimization at the industry level.

#### REFERENCES

- [1] E. Moshkbid, D. E. Cree, L. Bradford, and W. Zhang, "Biodegradable Alternatives to Plastic in Medical Equipment: Current State, Challenges, and the Future," *Journal of Composites Science*, vol. 8, no. 9, Sept. 2024, Art. no. 342, <https://doi.org/10.3390/jcs8090342>.
- [2] A. Patti and D. Acierio, "Towards the Sustainability of the Plastic Industry through Biopolymers: Properties and Potential Applications to the Textiles World," *Polymers*, vol. 14, no. 4, Feb. 2022, Art. no. 692, <https://doi.org/10.3390/polym14040692>.
- [3] H. Fu *et al.*, "Overview of Injection Molding Technology for Processing Polymers and Their Composites," *ES Materials & Manufacturing*, vol. 8, pp. 3–23, 2020, <https://doi.org/10.30919/esmm5f713>.
- [4] G. Pelin, M. Sonmez, and C.-E. Pelin, "The Use of Additive Manufacturing Techniques in the Development of Polymeric Molds: A Review," *Polymers*, vol. 16, no. 8, Apr. 2024, Art. no. 1055, <https://doi.org/10.3390/polym16081055>.
- [5] X. Li *et al.*, "Enhanced Thermal Properties of Polyamide 6, 6 Composite/Aluminum Hybrid via Injection Joining Strategy," *International Communications in Heat and Mass Transfer*, vol. 116, July 2020, Art. no. 104696, <https://doi.org/10.1016/j.icheatmasstransfer.2020.104696>.
- [6] A. Belkhir, "Controlling Glass/Matrix Interfacial Interactions Applied to In Situ Anionic PA6 Synthesis for Composite Manufacturing," Ph.D. dissertation, Department of Materials Science and Engineering, National Polytechnic Institute of Toulouse, Toulouse, France, 2022.
- [7] R. Kumar, S. K. Mishra, and S. Jayapalan, "Experimental Analysis on the Microstructural, Mechanical, Thermal and Tribological Properties of Graphene Nanoplatelets and Molybdenum Disulfide Filled Polyamide-6,6 Novel Hybrid Composite," *Polymer Composites*, vol. 46, no. 5, pp. 4703–4728, Apr. 2025, <https://doi.org/10.1002/pc.29270>.
- [8] R. Bertolini, A. Ghiotti, and S. Bruschi, "Machinability of Polyamide 6 Under Cryogenic Cooling Conditions," *Procedia Manufacturing*, vol. 48, pp. 419–427, 2020, <https://doi.org/10.1016/j.promfg.2020.05.064>.
- [9] M. Ovhall and P. Bharti, "Investigation of Optimization Machining Parameter for POM (Polyoxymethylene) while using TNMG Insert by Taguchi, ANOVA," *SSRN Electronic Journal*, 2023, <https://doi.org/10.2139/ssrn.4664300>.
- [10] H. Ying *et al.*, "Investigation of the Effect of the Cut Parameter on the Machining Performance of PTFE Cutting," *Journal of Manufacturing Processes*, vol. 103, pp. 144–155, Oct. 2023, <https://doi.org/10.1016/j.jmapro.2023.08.041>.
- [11] M. Aruna, "Optimization of Cutting Parameters in Machining Polyoxymethylene Using RSM," *IOP Conference Series: Materials Science and Engineering*, vol. 893, no. 1, July 2020, Art. no. 012005, <https://doi.org/10.1088/1757-899X/893/1/012005>.
- [12] A. I. Alateyah, Y. El-Taybany, S. El-Sanabary, W. H. El-Garaihy, and H. Kouta, "Experimental Investigation and Optimization of Turning Polymers Using RSM, GA, Hybrid FFD-GA, and MOGA Methods," *Polymers*, vol. 14, no. 17, Aug. 2022, Art. no. 3585, <https://doi.org/10.3390/polym14173585>.
- [13] M. Bozdemir, "Prediction of Surface Roughness considering Cutting Parameters and Humidity Condition in End Milling of Polyamide Materials," *Computational Intelligence and Neuroscience*, vol. 2018, pp. 1–7, June 2018, <https://doi.org/10.1155/2018/5850432>.
- [14] M. Abas *et al.*, "Experimental Investigation and Statistical Evaluation of Optimized Cutting Process Parameters and Cutting Conditions to Minimize Cutting Forces and Shape Deviations in Al6026-T9," *Materials*, vol. 13, no. 19, Sept. 2020, Art. no. 4327, <https://doi.org/10.3390/ma13194327>.
- [15] P. Quitiaquez, J. Cocha, W. Quitiaquez, and X. Vaca, "Investigation of Geometric Parameters with HSS Tools in Machining Polyamide 6 using Taguchi Method," *Materials Today: Proceedings*, vol. 49, pp. 181–187, 2022, <https://doi.org/10.1016/j.matpr.2021.08.002>.
- [16] P. Sidiq, R. M. Abdalrahman, and S. Rostam, "Optimizing the Simultaneous Cutting-Edge Angles, Included Angle and Nose Radius for Low Cutting Force in Turning Polyamide PA66," *Results in Materials*, vol. 7, Sept. 2020, Art. no. 100100, <https://doi.org/10.1016/j.rinma.2020.100100>.
- [17] M. A. Salman *et al.*, "Effect of Nozzle Diameter and Raster Angle on the Mechanical Properties of 3D Printed Nylon/ Carbon Fibers," *Engineering, Technology & Applied Science Research*, vol. 15, no. 2, pp. 21410–21417, Apr. 2025, <https://doi.org/10.48084/etasr.9979>.
- [18] W. H. A. Shaheen, M. Salman, R. A. Alaloosi, M. H. Tolephih, W. S. Abd Al-Sahb, and O. I. Abdullah, "Investigation of Effective Parameters on Oxygen Free High Conductivity Copper Deformation Based on Cutting Molds Design and Numerical Approach," *Advances in Science and Technology Research Journal*, vol. 19, no. 7, pp. 480–495, July 2025, <https://doi.org/10.12913/22998624/204303>.
- [19] E. Parodi, "Structure Properties Relations for Polyamide 6," Ph.D. dissertation, Department of Mechanical Engineering, Technische Universiteit Eindhoven, Eindhoven, Netherlands, 2017.
- [20] C. Hamzaçebi, "Taguchi Method as a Robust Design Tool," in *Quality Control - Intelligent Manufacturing, Robust Design and Charts*, P. Li, P. António Rodrigues Pereira, and H. Navas, Eds., IntechOpen, 2021.
- [21] J. Antony, *Design of Experiments for Engineers and Scientists*, 3rd ed. Edinburgh, Scotland, UK: Elsevier, 2023.
- [22] E. A. Ayyıldız, M. Ayyıldız, and F. Kara, "Optimization of Surface Roughness in Drilling Medium-Density Fiberboard with a Parallel Robot," *Advances in Materials Science and Engineering*, vol. 2021, no. 1, Jan. 2021, Art. no. 6658968, <https://doi.org/10.1155/2021/6658968>.
- [23] I. Sztankovics, "Study on the Roughness Parameters Describing Surface Functionality in Bore Honing," *Multidiszciplináris Tudományok*, vol. 13, no. 2, pp. 135–143, Dec. 2023, <https://doi.org/10.35925/j.multi.2023.2.12>.